Indian Journal of Biochemistry & Biophysics
Vol. 59, March 2022, pp. 320-330

# Cloning and structural elucidation of a brassinosteroids biosynthetic gene (*Atdwarf*4) and genetic transformation of Indian mustard (*Brassica juncea* L.)

Hay V Duong[1,2†], Sai Krishna Repalli[1†], Payal Gupta[1†], Rohini Sreevathsa[1], Devendra K Yadava[3] & Prasanta K Dash[1]*

[1]ICAR-National Institute for Plant Biotechnology, Pusa Campus, New Delhi-110 012, Delhi, India

[2]Bioenviromental Chemistry, Jeonbuk National University, Jeonju-54896, Republic of Korea

[3]ICAR-Indian Agricultural Research Institute, New Delhi-110 012, Delhi, India

*Received 22 December 2021*; *revised 10 February 2022*

Phytohormones play critical roles in plant growth and development. Brassinosteroids (BRs) are essential group of phytohormones required for optimum growth of plants and their deficiency causes distinctive dwarf phenotypes in plants. Homeostasis of BRs in plants is maintained by DWARF4 enzyme that mediates multiple 22α-hydroxylation steps in brassinosteroid biosynthesis. *Arabidopsis* plants over-expressing DWARF4 show increase in inflorescence, number of branches and siliques; thereby increased number of seeds/plant. This suggests that engineering DWARF4 biosynthesis in *Brassica* plant can be strategized to enhance yield in mustard. In the present study (i) we cloned *dwarf4* gene from *Arabidopsis* using gene specific PCR strategy, (ii) elucidated the three-dimensional structure of DWARF4 protein at molecular level where it revealed presence of four beta sheets and 20 alpha-helices, and (iii) transformed mustard cultivar Pusa Jaikisan with an objective to develop transgenic mustard with enhanced number of siliques. We obtained several putative transgenics with an average transformation efficiency of 3.3%. Molecular characterization with *nptII* specific primers confirmed presence of transgene in six putative transgenic plants.

**Keywords**: Three-dimensional structure, Brassinosteroids, Cloning, Genetic transformation, Mustard, Phytohormones, Regeneration

Phytohormones (or plant growth regulators) are chemical compounds that are synthesized by plants to control growth and development. They play crucial roles in cellular metabolism such as regulated cell division, elongation, and differentiation[1]. Besides the canonical hormones, such as auxins, cytokinins and gibberellins; brassinosteroids (BRs) are implicated as important plant growth hormone. The discovery of brassinosteroids dates back to nearly a hundred and fifty years, when the role of brassinosteroids in photomorphogenesis/shade avoidance response was identified in classical buckwheat experiments in 1863. Brassinosteroid was first isolated as an organic extract nearly fifty years ago from the pollen of *Brassica napus* that showed growth promoting properties and was termed as "Brassin"[2]. Amongst all BRs, Brassinolide (BL), the biologically most active BR, was isolated from *Brassica* pollen extract[3]. BRs are ubiquitous in the plant kingdom[4] and seventy compounds with similar BR activity have been extracted from various plant sources.

BRs are involved in cell elongation, cell division, vascular system differentiation, senescence, and stress tolerance[5,6]. BR signal transduction and BR biosynthesis pathways have been uncovered within the last two decades[7]. The biological importance of BRs has been reinforced by the characterization of a variety of mutants perturbed in signaling or biosynthesis of this hormone[1].

In *Arabidopsis*, molecular genetic analysis of BR-deficient mutants have elucidated the involvement of several BR biosynthetic genes. Amongst the cascades of biosynthetic genes, *dwarf1* was first cloned[8] by reverse genetics approach. Currently, eight BR dwarf loci in *Arabidopsis* have been identified *viz*. *dwarf1* to *dwarf*8 while *dwarf*4 has been proposed to be a key enzyme that determines flux of BR biosynthesis[9]. When its expression is completely knocked out, it resulted in severe growth defects due to deficiency in synthesis of bioactive BR[10]. Conversely, increased flux of BR biosynthesis by over-expression of *dwarf4* resulted in a completely opposite phenotype. All the examined organs such as

†Equal first author
*Correspondence:
Phone: 25841787; Fax: 25843984
E-mail: prasanta01@yahoo.com

petioles, pedicels, inflorescences, and leaf blades were elongated, and seed yield was noticeably increased in *Arabidopsis*[11]. In addition, accumulating data suggest that BRs are responsible for light-dependent regulation of plant growth[12]. In fact, feeding studies utilizing BR intermediates showed that only 22α-hydroxylated BRs rescued the *dwarf4* phenotype, confirming that *dwarf*4 acts as a 22α-hydroxylase[9] which is a key enzyme in the rate limiting step of BR biosynthesis. In addition, Shimada *et al*., (2003) showed that BR biosynthetic genes, such as *dwarf*4 are also feedback regulated by exogenous BRs[13]. *dwarf*4 expression is curbed by exogenous application of BL, suggesting *dwarf*4 expression may serve as a focal point in the quantitative regulation of endogenous bioactive BR levels[14].

With the decoding of molecular mechanisms affecting the yield component in crops through genomics[15–17] and transgenics[18, 19]; it is now possible to over-express intrinsic yield genes to increase grain number or alternative approaches to impart biotic/abiotic[20–22] tolerance or engineer a trait in crops[23]. Keeping in view the cardinal role played by *dwarf*4 gene in BR biosynthesis and its regulatory action in metabolic flux including cell elongation, photomorphogenesis and yield, the present investigation focused on isolation, cloning, molecular characterization, three-dimensional structure prediction of DWARF4 protein and transformation of Pusa Jaikisan, a high yielding Indian variety of *Brassica* with *Atdwraf*4 gene to enhance seeds per silique and siliques per inflorescence.

## Materials and Methods

### Plant material and PCR amplification *Atdwarf4*

Seeds of *Brassica juncea* var. Pusa Jaikisan were procured from Division of Genetics, IARI (New Delhi) and *Arabidopsis* Col0 seeds were available in the laboratory. Genomic DNA was isolated from shoot tissue of *Arabidopsis* plants using CTAB method[24]. *Atdwarf4* gene was cloned using gene specific PCR based strategy[25-29]. The *dwarf4* gene was PCR amplified from *Arabidopsis* genomic DNA, in a 50 µL reaction volume containing sterilized pure water (40 µL), 5× PCR buffer (5 µL), 0.2 mM of each of forward and reverse primers, 0.2 mM of dNTPs mix, phusion Taq polymerase (1.25 U) and 100 ng of template DNA. Amplification was performed in PCR cycler with the following cycling conditions: an initial denaturation of template DNA at 98°C for 30 sec followed by 30 cycles of amplification *i.e*., 10 sec denaturation at 98°C, 20 sec primer annealing at 60°C, and 30 sec primer extension at 72°C and 10 min final extension at 72°C. The forward and reverse primers were designed using PRIMER 3 tool and the primer sets used for gene amplification, *viz*, *dwarf*4FP: **CACC**AACTAGCTCCATGTTCGAAACAG and *dwarf*4RP: CAGAATACGAGAAACCCTAATAG. Gateway cloning site (CACC, bold sequence) was added to the 5′ end of forward primer to aid gateway cloning. Purified PCR products were analysed on 1.2% agarose gel for its quality and quantity.

### Cloning of *Atdwarf4* gene

PCR amplified *dwarf*4 gene was cloned using gateway cloning technology and was subsequently mobilized to pK7FWG2 (destination vector) as per the manufacturer's protocol. In brief, *dwarf4* gene was cloned in pENTR/SD/TOPO (entry vector), using BP reaction and transformed into chemically competent DB3.1 cells. The recombinant colonies (white) obtained after overnight incubation at 37°C were picked and streaked onto fresh LA + Kanamycin (50 µg/mL) plates.

Recombinant clones (Fig. 1A) were confirmed by colony PCR with gene specific primers and restriction digestion with *Bam*HI/*Hin*dIII enzymes. The PCR amplified products and restricted DNA samples were analyzed on 1.2% agarose gel. The complete nucleotide sequence was determined by sanger di-deoxy sequencing. pENTR/SD/TOPO vector based sequencing primers, universal forward and reverse (M13F and M13R) primers were used for sequencing. *dwarf4* gene specific primers were also used for confirming the sequence. The final sequence was determined from both strands and comparison of *Atdwarf4* nucleic acid and amino acid sequences with already existing sequences was performed.

In the second step, entry vector containing the *dwarf4* gene was used to mobilize the *dwarf4* gene into pK7FWG2 vector (binary vector) using LR clonase reaction as per manufacturer's protocol. 1 µL of LR clonase reaction was transformed into DB3.1 *E. coli* cells and colonies were selected on LA + Spectinomycin (50 µg/mL) plates. Recombinant clones (Fig. 1B) were confirmed by restriction with *Hind*III enzyme. Putative recombinant clones were re-sequenced with gene specific primers and recombinant clone carrying *dwarf4* gene was mobilized into *Agrobacterium* strain GV3101 by freeze thaw method[30].

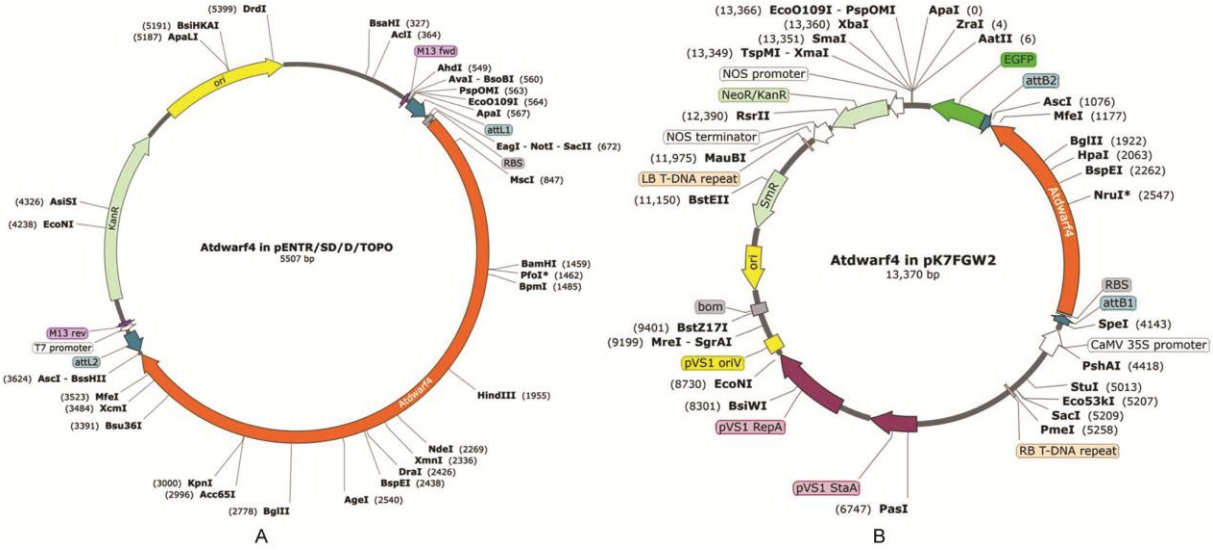


Fig. 1 — Vector maps of *Atdwarf4*. (A) *Atdwarf4* in pENTR/SD/TOPO sub-cloning vector; and (B) *Atdwarf4* in pK7FWG2 binary vector

**Structure prediction and validation of *At*DWARF4**

Three-dimensional structure of DWARF4 protein was predicted by the method of Dash *et al*[25]. Model of DWARF4 was constructed using I-TASSER server (http://zhanglab.ccmb.med.umich.edu/I-TASSER/)[31]. Other online models have also been used for structure prediction[32–34] but I-TASSER (as 'Zhang-Server') was ranked as the No 1 server for protein structure prediction. I-TASSER (Iterative Threading ASSEmbly Refinement) is a hierarchical approach to protein structure and function prediction. Structural templates are first identified from the PDB by multiple threading approach; full length atomic models are then constructed by iterative template fragment assembly simulations. The generated model was refined using ModRefiner (http://zhanglab.ccmb.med. umich.edu/ModRefiner/) that uses the algorithm for high- resolution protein structure refinement. Further, discrete molecular dynamic simulation of refined structure was performed to remove steric clashes and reduced van der waals repulsion forces. The stereo-chemical properties of DWARF4 were assessed by Ramachandran plot analysis[35]. Validation of the modelled structure was performed using SAVES server and PDBsum[36]. Structure visualization was performed using Pymol. The predicted model of protein was submitted to Protein Model DataBase[37] (http://srv00.recas.ba.infn.it/ PMDB/main.php).

**Transformation of *Atdwarf4* gene into *Brassica***

Seeds of *Brassica juncea* cv. Pusa Jaikisan were surface sterilized with a drop of Tween-20 and 70% ethanol for 3 min followed by 0.1% mercuric chloride for 3-4 mins with intermittent washing with autoclaved double distilled water at every step. The sterilized seeds were germinated on half strength MS medium to raise seedlings and cotyledonary nodes were excised from the seven-day-old seedlings and inoculated on MS medium[38]. After 3 days they were infected with *Agrobacterium* GV3101 strain harboring *Atdwarf4* gene and placed in co-cultivation medium (MS medium supplemented with BAP (4 mg $L^{-1}$) and $AgNO_3$ (3.5 mg $L^{-1}$) for 3 days and later transferred to selection medium (MS medium supplemented with BAP (4 mg $L^{-1}$), Cefotaxime (250 mg $L^{-1}$), $AgNO_3$ (3.5 mg $L^{-1}$) and Kanamycin (50 mg $L^{-1}$). The selection was repeated for 3 cycles with sub-culturing for every 10 days. Actively growing shoots were selected at each stage and transferred into regeneration medium (MS medium supplemented with BAP (4 mg $L^{-1}$), Cefotaxime (250 mg $L^{-1}$), AgNO3 (3.5 mg $L^{-1}$) and Kanamycin (50 mg $L^{-1}$). They were grown for one month until healthy shoots were formed. Healthy shoots were then transferred to rooting medium (MS medium supplemented with NAA (1 mg $L^{-1}$) for the development of roots.

**Molecular characterization of putative transgenics**

Genomic DNA was isolated from rooted putative transgenics and untransformed control plants by CTAB method[24]. The genomic DNA was purified and then subjected to PCR analysis by using *nptII* forward and reverse primer. Each reaction tube contained 10x PCR buffer, 0.2 mM of each forward and reverse

primers, 0.2 mM of dNTPs mix, Taq polymerase (1.25 U) and 100 ng of template DNA. Amplification was performed in a Thermal cycler with following cycling conditions: an initial denaturation of template DNA at 94°C for 3 minutes followed by 30 cycles of amplification *i.e*., 30 sec denaturation at 94°C, 30 sec primer annealing at 60°C, and 1 min primer extension at 72°C and 10 min final extension at 72°C. PCR products were assessed on 1.2% agarose gel.

## Results

### Cloning and confirmation of *Atdwarf4* gene

PCR amplification of *Atdwarf4* gene from the genomic DNA of *Arabidopsis* template resulted in a fragment of 2.9 kb (Fig. 2). The amplified PCR product containing gateway compatible CACC site was ligated to pENTR/SD/TOPO control vector. The ligated mixture was transformed into *E. coli* DB3.1 competent cells. Five randomly picked colonies were used for colony PCR to check the presence of the *dwarf*4 gene (Fig. 3A). Presence of *dwarf*4 gene was further confirmed by restriction digestion with *Hin*dIII/*Eco*RI enzymes that released the expected fragment of ~500bp (Fig. 3 B). Similarly, cloning of *dwarf4* gene in binary vector pK7FWG2 was confirmed by restriction digestion with *Hin*dIII enzyme. Recombinant clones generated a fragment of ~ 2.5 kb upon restriction with *Hin*dIII (Fig. 3C).

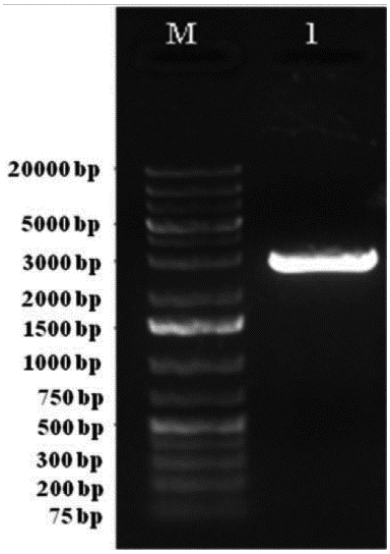


Fig. 2 — PCR Amplification of *dwarf4* gene from *Arabidopsis* genomic DNA. Lane M-: 1 kb plus ladder; Lane 1: *Atdwarf4* gene amplified from *Arabidopsis* genomic DNA

Sanger sequencing of the cloned *dwarf*4 gene revealed the size to be of 2.9 kb. Based on the blast results; the *dwarf4* gene was found to be a full-length gene coding for 513 amino acids. The cloned *dwarf*4 gene showed 100% homology with *Arabidopsis* DWARF4 and 93% homology with the rice cytochromeP450 indicating a common descent (Fig. 4).

### 3D structure analysis

For detailed structural analysis three-dimensional structure of cloned DWARF4 protein was deduced using 513 amino acids sequence by using i-TASSER server. The homology modelled initial structure was based on template crystal structure of *Arabidopsis thaliana* CYP90B1 in complex with cholesterol (PDB entry 6A15)[39]. DWARF4 model had a C-score of −0.36 and a TM score of 0.67±0.13.

This initial model was refined using Modrefiner and Ramachandran plot analysis that revealed only 90.4%

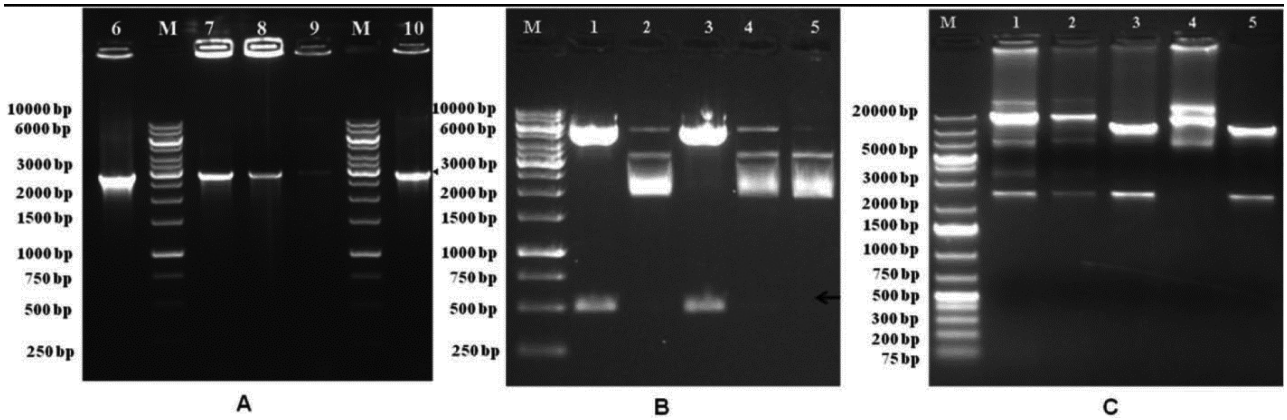


Fig. 3 — Confirmation of cloned *Atdwarf*4 gene in entry vector and binary vector. (A) Colony PCR confirmation of *Atdwarf*4 gene. Lane M: 1 kb ladder. Lane 6, 7, 8, 9, 10: positive ~2.9 kb amplification of *dwarf*4 gene; (B) Restriction digestion confirmation of *dwarf4* gene in entry vector. Lane M: 1 kb ladder. Lane 1-5: Putative *dwarf4* gene in pENTR/SD/TOPO vector restricted with *Bam*HI and *Hind*III. Positive clones (Lane 1, 3) released a fragment of ~500 bp upon double digestion with *Bam*HI and *Hind*III; and (C) Cloning of *dwarf4* into binary vector pK7FWG2 and confirmation by restriction digestion. Lane M: 1 kb plus ladder. Lane 1-5: Putative *dwarf4* gene in pK7FWG2 restricted with *Hin*dIII enzyme. Positive clones (lane1, 3, 5) released a fragment of ~ 2.5 kb on restriction with *Hin*dIII

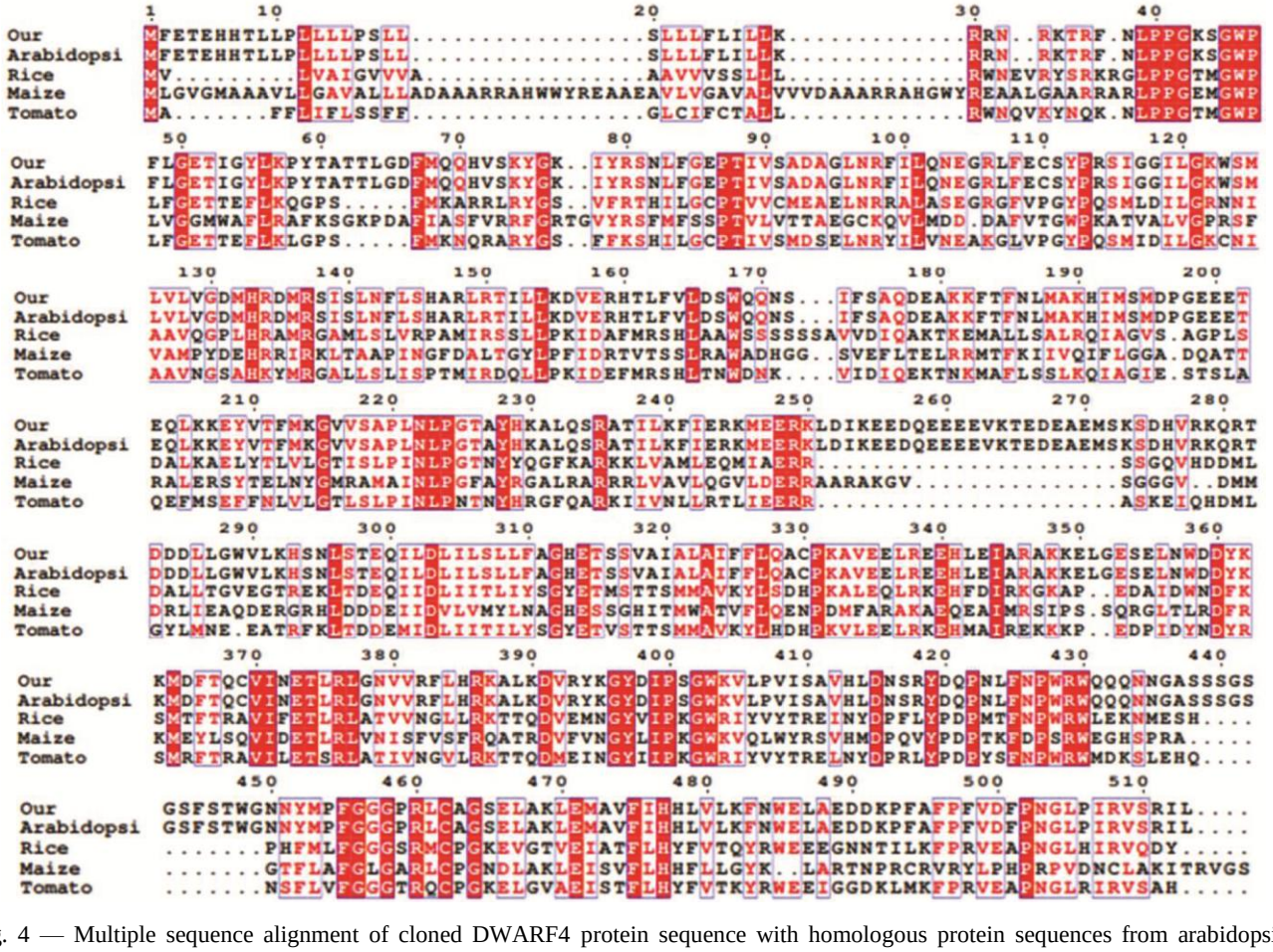


Fig. 4 — Multiple sequence alignment of cloned DWARF4 protein sequence with homologous protein sequences from arabidopsis, tomato, rice, and maize

residues in favoured region, but 2% residues were in outlier region. Further, the initial model was iteratively re-refined using Modloop until 0% residues fell in the outlier region with 95.9% residues in favoured region and 4.1% in the allowed region (Fig. 5). The quality of final refined model was evaluated through SAVES server using PROCHECK, Verify-3D program that focused on backbone conformation and its geometric properties, nature of residual interaction etc. While PROCHECK evaluated the reliability of torsion angle Φ, Ψ and quantified the number of allocated residues, the refined model showed 95.9% residues in the favoured region and 4.1% of residues in allowed region with no residues in the disallowed/outlier region of the plot. The predicted model was submitted to Protein Model DataBase (PMDB) and was assigned the identifier #PM0084199.

The 3D–model predicted by homology modelling was validated by PDBsum. DWARF4 structure (Fig. 6) revealed the presence of four beta sheets and 20 alpha-helices. β-sheet A contained five mixed type β-strands with topology 1 3X -1 -1, sheet B contained one mixed type β-strand, sheet C contained three antiparallel type β-strands with -2x 1 topology and sheet D contained two antiparallel type β-strands with 1 topology. The protein also contained 20 α-helices *viz*; α1 {Leu21-Arg31(11 residues)}, α2 {Thr52-Leu56 (5 residues)}, α3{Gln69-Tyr75(7 residues)}, α 4{Ala94-Gln102(9 residues)}, α5{Ser115-Gly118 (4 residues)}, α6{Gly130-Asn142(13 residues)}, α7{His146-Ser167(22 residues)}, α8{Ala176-Ile192 (17 residues)}, α9 {Glu199-Ser218(20 residues)}, α10 {Thr226-Glu255(30 residues)}, α11{Glu259-Glu262 (4 residues)}, α12 {Asp283-Val290(8 residues)}, α13{Thr298-Ala329(32 residues)}, α14{Pro331-Leu351(21 residues)}, α15{Trp358-Lys363 (6 residues)}, α16{Asp365-Gly378(14 residues)}, α17{Ile409-Leu414 (6 residues)}, α18{Pro427-Arg429(3 residues)}, α19{Gly458-Arg460 (3 residues)} and α20{Ser465-Lys482 (18 residues)}. 3 β-hairpins of classes 2:4, 2:2 IP and 17:19 were identified[40]. Two beta-buldges of anti-parallel G1 type and 11 strands

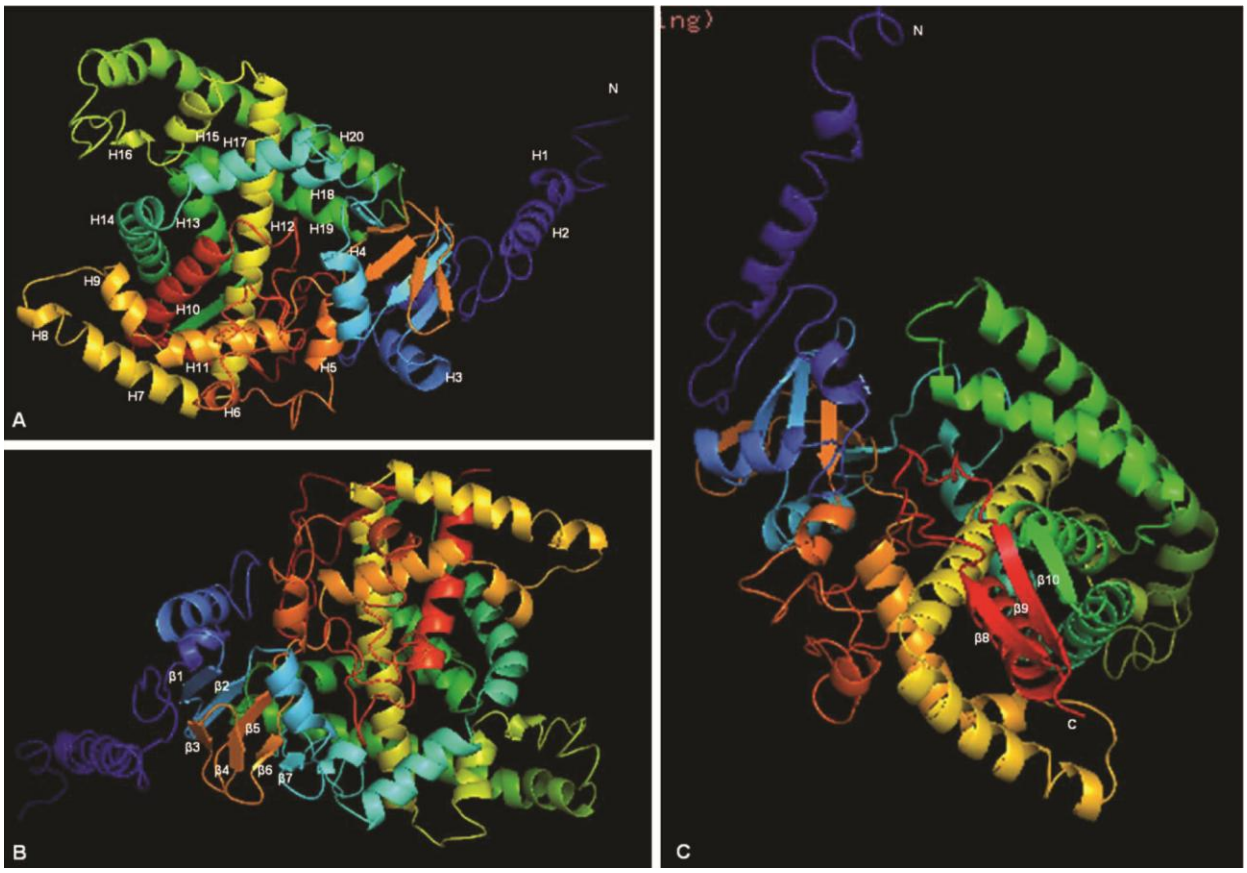


Fig. 5 — Three-dimensional structure of DWARF4 from *Arabidopsis*. *A* Stereo-ribbon diagram of the DWARF4 monomer (chain A) color-coded from the N-terminus (blue) to the C-terminus (red). Helices (H1–H20) and β-strands (β1–β10) are indicated. (A), (B), and (C) are different views of predicted structure

were identified. Thirty helix-helix interactions of H-H type were identified. One β-α-β motifs with 26 loops and 11 helices participations were identified along with one β-bulges anti-parallel wide type was also identified. There are 81 β-turns in total belonging to 4 classes: I, II, IV and VIII[41]. Twelve γ turns, nine inverse type and three classic type were also recognized. Apart from these, three pores and nine tunnels were also identified (Fig. 6).

***Agrobacterium*-mediated transformation of *Brassica***

*Agrobacterium* strain GV30101 containing *dwarf*4 gene in pK7FWG2 vector was used to transform mustard variety Pusa Jaikisan. Green shoots on Kanamycin plates were assumed to be putative transgenics. Such shoots were excised and transferred to bottles containing MS + NAA (1 mg $L^{-1}$) + Cefotaxime (250 mg $L^{-1}$) + Kanamycin (25 mg $L^{-1}$) for rooting (Fig. 7). However, during the screening many such putative plants bleached out and only eight plants survived on rooting media after several sub-cultures. Two out of eight plants could not acclimatize during hardening. Therefore, molecular confirmation was performed for six plants which survived the process of hardening. Altogether, ten batches of transformation were carried out. However, regeneration efficiency varied amongst ten batches with an average regeneration efficiency of 7.697% (Table. 1). Highest regeneration efficiency was observed in the first batch followed by third, sixth and second batch, with more than 10% regeneration efficiency. While, the eighth batch showed regeneration efficiency of 8.5%, the remaining batches showed less than 5% regeneration. However, the explants of fourth batch did not survive at all due to unknown reasons (Table. 1).

The average transformation efficiency was observed to be 3.3%. Transformation efficiency of each batch varied depending on the number of explants inoculated and number of explants that regenerated green shoots (excluding chimeric shoots) in first selection cycle and number of green shoots that survived on the successive sub-culture in selection medium. It was 2.3, 5.6 and 25.0

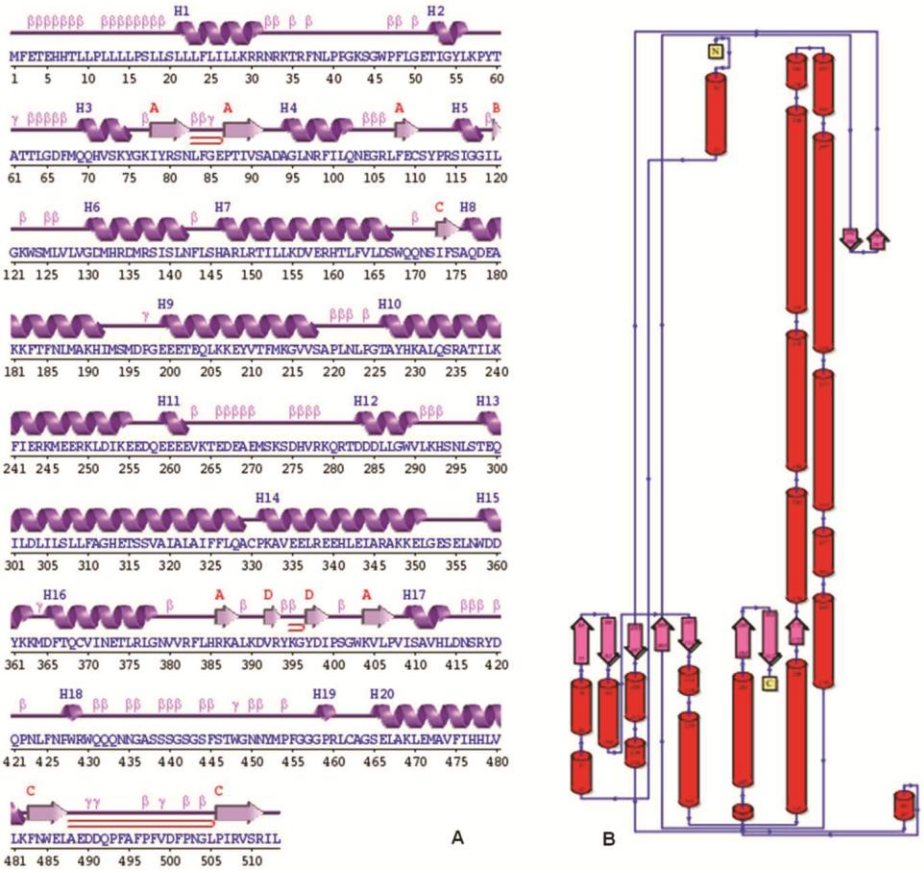


Fig. 6 — (A) Diagram showing the secondary-structure elements of DWARF4 superimposed on its primary sequence. The labelling of secondary-structure elements is in accordance with PDBsum (http://www.ebi.ac.uk/pdbsum): α-helices are labelled H1 – H20, the β-strands are labeled β1–β11, β-turns and γ-turns are designated by their respective Greek letters (β, γ) and red loops indicate β-hairpins. (B) Topology of DWARF4 protein showing the orientation of α-helices and β-strands

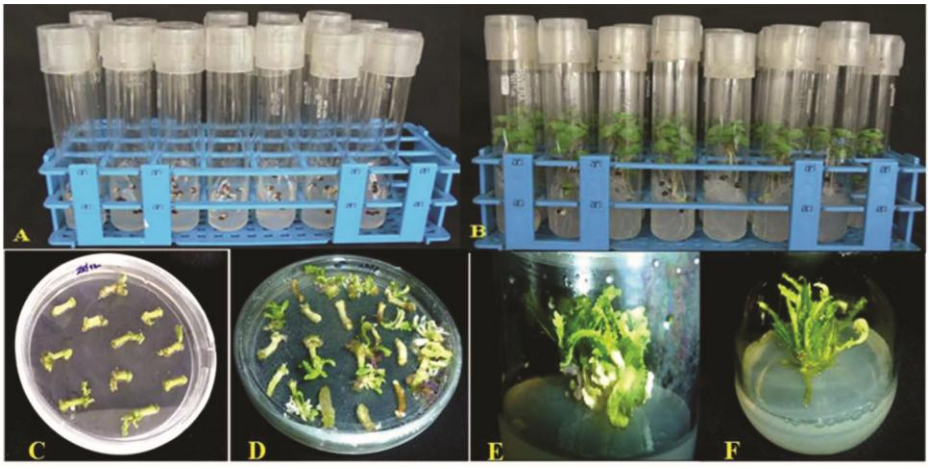


Fig. 7 — Stepwise procedure of transformation of mustard with *Atdwarf4* gene construct. (A) Sterilized seeds germinated on ½ MS media; (B) Mustard seedlings on 6th day after inoculation on MS media; (C) Selection and regeneration of the transformed shoots on MS + BAP (4 mg $L^{-1}$), Cefotaxime (250 mg $L^{-1}$), AgNO3 (3.5 mg $L^{-1}$, ) and Kanamycin (50 mg $L^{-1}$) at the end of 3 weeks; (D) Selection and regeneration of the transformed shoots on MS + BAP (4 mg $L^{-1}$), Cefotaxime (250 mg $L^{-1}$), AgNO3 (3.5 mg $L^{-1}$, ) and Kanamycin (50 mg $L^{-1}$) at the end of 5 weeks; (E) Organogenesis in transformed *Brassica* explants in shooting medium with MS + BAP (4 mg $L^{-1}$), Cefotaxime (250 mg $L^{-1}$), AgNO3 (3.5 mg $L^{-1}$) and Kanamycin (50 mg $L^{-1}$); and (F) Root induction in transformed *Brassica* explants in rooting medium with MS + NAA(1 mg $L^{-1}$)

Table 1 — Batch wise regeneration efficiency of transformed explants

| Batch No | No. of explants inoculated (7 days) (a) | No. of explants | | Regeneration efficiency (%) (b-c)/a x 100 |
|---|---|---|---|---|
| | | Forming green shoots (30-35 days) (b) | Forming chimeric shoots (30-35 days) (c) | |
| 1 | 289 | 52 | 6 | 15.91 |
| 2 | 205 | 28 | 2 | 12.68 |
| 3 | 192 | 48 | 18 | 15.62 |
| 4 | 300 | 20 | 20 | 0.00 |
| 5 | 235 | 39 | 37 | 0.85 |
| 6 | 269 | 39 | 3 | 13.38 |
| 7 | 293 | 46 | 36 | 3.41 |
| 8 | 247 | 33 | 12 | 8.50 |
| 9 | 275 | 29 | 20 | 3.27 |
| 10 | 239 | 38 | 30 | 3.35 |

Table 2 — Batch wise transformation efficiency in mustard

| Batch No | No. of regenerated shoots on selection medium (55-60 days) | Plants chimeric on selection medium (80-90 days) | Plants transferred to rooting medium (95 days) | Transformation Efficiency (%) |
|---|---|---|---|---|
| 1 | 64 | 64 | 0 | 0 |
| 2 | 37 | 37 | 0 | 0 |
| 3 | 85 | 83 | 2 | 2.4 |
| 4 | 0 | 0 | 0 | 0 |
| 5 | 4 | 4 | 0 | 0 |
| 6 | 72 | 68 | 4 | 5.6 |
| 7 | 18 | 18 | 0 | 0 |
| 8 | 40 | 40 | 0 | 0 |
| 9 | 9 | 9 | 0 | 0 |
| 10 | 8 | 6 | 2 | 25.0 |

percent in third, sixth and tenth batch respectively (Table. 2). However, due to consecutive stringent selection cycles maintained for every 10 days, regenerated shoots did not survive on the selection medium and eventually transformation efficiency was zero for rest of the batches and overall average transformation efficiency for all the ten batches was observed to be 3.3%. Representative explants during different stages of tissue culture from seed inoculation, germination, selection, regeneration and rooting are shown in (Fig. 7).

#### Molecular characterization of putative transgenics

We obtained eight putative transgenic plants after stringent selection and transferred them for successful rooting. However, six putative transgenic plants survived during the process of hardening after repeated sub-culture and molecular characterization was carried out using these six putative plants. The DNA was isolated from the shoot and PCR was carried out using *nptII* specific primer. Plasmid DNA containing *dwarf4* in pK7FWG2 vector was used as positive control (P) and for negative control, untransformed (NT) mustard DNA was used. An amplicon size of 760 bp with respect to that of *nptII* gene was obtained through PCR. The amplification products were similar in size to the products obtained in the positive control (plasmid), while no amplification was detected in the non-transformed plants (Fig. 8). All the six plants (1-6) were PCR positive (Fig. 8) confirming transformation of mustard plants.

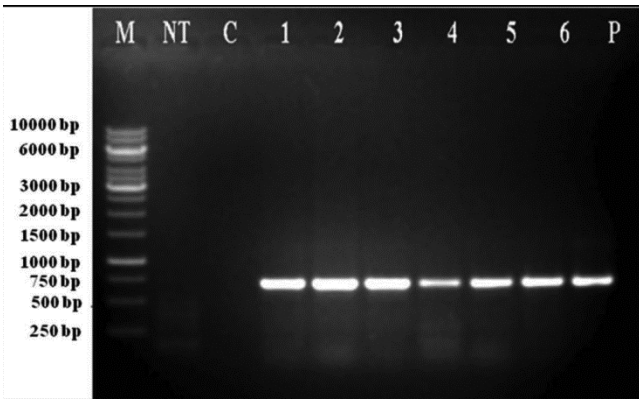


Fig. 8 — PCR confirmation of *nptII* gene in the putative mustard plants. Lane M: 1 Kb ladder, NT: Untransformed mustard (−ve) control, C: PCR without template (−ve control), 1-6: six putative transgenics containing *Atdwarf4-nptII*, P: plasmid containing *Atdwarf4-nptII* (+ ve control)

## Discussion

Green revolution focused on priority crops (rice and wheat) that served as staple food for the mankind[42,43]. Mustard (*Brassica juncea* L.) is the third important oilseed crop in the world and second important oilseed crop in India[44]. Like all field crops, yield in mustard depends on physiological status of plants including homeostasis of phytohormones. Brassinosteroids (BRs) are a class of polyhydroxyl steroidal hormones which play critical roles in multiple physiological processes during normal plant growth and development, from seed germination to leaf senescence. In *Arabidopsis*, BR biosynthesis occurs in a multistep pathway and an important rate-limiting step in the BR biosynthetic pathway is governed by *dwarf4* gene encoding DWARF4 enzyme. The DWARF4 enzyme mediates multiple 22α-hydroxylation steps in brassinosteroid biosynthesis. *Arabidopsis* plants over-expressing

*dwarf4* gene[11] showed two-fold increase in inflorescence, branches and siliques. This massive increase led to 59% increase in the number of seeds produced/plant. Thus, it suggests that it is possible to enhance seed yield in mustard by engineering DWARF4 and BR biosynthesis in mustard.

Our study involved over-expression of *Atdwarf4* gene in Indian mustard variety, Pusa Jaikisan. This cultivar was chosen for tissue culture experiments keeping in view the amenability of the variety for tissue culture response. In our endeavour, we successfully cloned 2.9 kb *dwarf*4 gene using gene specific primers from arabidopsis. The translated nucleotide sequence comprised of 513 amino acids including the start codon. This is consistent with the earlier reports of *Atdwarf*4 isolation and cloning[45]. *dwarf4* gene has internal restriction sites for *Hin*dIII and *Eco*RI at 1469 and 1960 bp. Thus, upon restriction, an expected 500bp fragment confirmed the cloning of *dwarf4* into entry vector. Since, the target gene was amplified from arabidopsis genome, to rule out the false priming of gene and/or inadvertent truncation of the gene, cloned *dwarf*4 was Sanger sequenced. Complete homology (100%) in sequence of cloned *dwarf*4 (Fig. 4) proved it as a *bonafide* full-length *dwarf4* gene and is devoid of any PCR generated mutation.

The 3D structure of DWARF4 protein, predicted using I-TASSER server was based on template crystal structure of *Arabidopsis thaliana* CYP90B1 in complex with cholesterol (PDB entry 6A15)[39]. DWARF4 shared all the features of cytochrome P450 monooxygenase (CPYs) with *Arabidopsis* such as catalysing the 22 (S)-hydroxylation of campesterol which is the first and rate-limiting enzyme at the branch point of the biosynthetic pathway from sterols to BRs[46]. DWARF4 model had C-score of -0.36 indicating a good quality model. C-score ranged from −5 to 2 and a higher value indicating high quality of the model. TM-score >0.5 indicated a model of correct topology and a TM-score <0.17 meant a random similarity. A TM score of 0.67±0.13 for DWARF4 was indicative of correct topology. Also, occurrence of >90% residues (95.9% residues) in favoured region of Ramachandran plot signified the stereochemical stability of the generated and refined molecule. The 3D structure was validated by PDBsum.

*Agrobacterium* strain GV30101 containing the *dwarf*4 in pK7FWG2 vector was used to transform Pusa Jaikisan. After initial co-cultivation with *Agrobacterium*, transformed explants were regenerated on MS + BAP (4 mg $L^{-1}$) + Kanamycin (50 mg $L^{-1}$) selection plates. Kanamycin was used as plant selection marker as the binary vector contained *npt*II gene in its T-DNA region. Successive batches of cotyledonary nodes were transformed and chimeric or albinos were eliminated from selection. The average transformation efficiency was 3.3% from a set of ten batches. After repeated sub-cultures, we obtained six plants that rooted and these plants tested positive for presence of *nptII* gene.

## Conclusion

We focused on cloning *dwarf4* gene from *Arabidopsis* and genetically transforming it into mustard plants (*Brassica juncea* var. Pusa Jaikisan) for increased seed yield. We were partially successful in developing putative transgenic in mustard with average transformation efficiency of 3.3%. Additionally, we predicted the three-dimensional structure of DWARF4 protein to get an insight into its structure and function for leveraging the potential of *dwarf*4 gene for enhanced yield in mustard by tinkering BRs homeostasis.

## Acknowledgement

Present study was supported in the form of in-house and DBT-twinning projects to PKD by Indian Council of Agricultural Research (ICAR) and DBT, Govt. of India, New Delhi, India. This is NIPB Publication No Res/2022/24.

## Conflicts of interest

All authors declare that there is no conflict of interest.

## References

1 Fridman Y, Strauss S, Horev G, Ackerman-Lavert M, Reiner-Benaim A, Lane B, Smith RS & Savaldi-Goldstein S, The root meristem is shaped by brassinosteroid control of cell geometry. *Nat Plants*, 7 (2021) 1475.

2 Mitchell JW, Mandava N, Worley JF, Plimmer JR & Smith MV, Brassins—a new family of plant hormones from rape pollen. *Nature*, 225 (1970) 1065.

3 Grove MD, Spencer GF, Rohwedder WK, Mandava N, Worley JF, Warthen JD, Steffens GL, Flippen-Anderson JL & Cook JC, Brassinolide, a plant growth-promoting steroid isolated from Brassica napus pollen. *Nature*, 281 (1979) 216.

4 Somssich M, Vandenbussche F, Ivakov A, Funke N, Ruprecht C, Vissenberg K, VanDer Straeten D, Persson S & Suslov D, Brassinosteroids influence *Arabidopsis* hypocotyl graviresponses through changes in mannans and cellulose. *Plant Cell Physiol*, 62 (2021) 678.

5 Choe, *Brassinosteroid biosynthesis and metabolism. Plant Hormones: Biosynthesis, Signal transduction*. (Kluwer Academic Publishers) 2004.

6 González-García MP, Vilarrasa-Blasi J, Zhiponova M, Divol F, Mora-García S, Russinova E &Caño-Delgado AI, Brassinosteroids control meristem size by promoting cell cycle progression in *Arabidopsis* roots. *Development*, 138 (2011) 849.

7 Kim TW & Wang ZY, Brassinosteroid signal transduction from receptor kinases to transcription factors. *Annu Rev Plant Biol*, 61 (2010) 681.

8 Feldmann KA, Marks MD, Christianson ML & Quatrano RS, A dwarf mutant of *Arabidopsis* generated by T-DNA insertion mutagenesis. *Science*, 243 (1989) 1351.

9 Choe S, Dilkes BP, Fujioka S, Takatsuto S, Sakurai A & Feldmann KA, The *DWF4* gene of *Arabidopsis* encodes a cytochrome P450 that mediates multiple 22α-hydroxylation steps in brassinosteroid biosynthesis. *Plant Cell*, 10 (1998) 231.

10 Vukašinović N, Wang Y, Vanhoutte I, Fendrych M, Guo B, Kvasnica M, Jiroutová P, Oklestkova J, Strnad M & Russinova E, Local brassinosteroid biosynthesis enables optimal root growth. *Nat Plants*, 7 (2021) 619.

11 Choe S, Fujioka S, Noguchi T, Takatsuto S, Yoshida S & Feldmann KA, Overexpression of DWARF4 in the brassinosteroid biosynthetic pathway results in increased vegetative growth and seed yield in *Arabidopsis*. *Plant J*, 26 (2001) 573.

12 Kang JG, Yun J, Kim D-H, Chung KS, Fujioka S, Kim JI, Dae HW, Yoshida S, Takatsuto S, Song PS & Park CM, Light and brassinosteroid signals are integrated via a dark-induced small G protein in etiolated seedling growth. *Cell*, 105 (2001) 625.

13 Shimada Y, Goda H, Nakamura A, Takatsuto S, Fujioka S & Yoshida S, Organ-specific expression of brassinosteroid-biosynthetic genes and distribution of endogenous brassinosteroids in *Arabidopsis*. *Plant Physiol*, 131 (2003) 287.

14 Chaiwanon J & Wang ZY, Spatiotemporal brassinosteroid signaling and antagonism with auxin pattern stem cell dynamics in *Arabidopsis* roots. *Curr Biol*, 25 (2015) 1031.

15 Dash PK, Cao Y, Jailani AK, Gupta P, Venglat P, Xiang D, Dash PK, Cao Y, Jailani AK, Gupta P, Venglat P, Xiang D, Rai R, Sharma R, Thirunavukkarasu N, Abdin MZ, Yadava DK, Singh NK, Singh J, Selvaraj G, Deyholos M, Kumar PA & Datla R, Genome-wide analysis of drought induced gene expression changes in flax (*Linum usitatissimum*). *GM Crops Food*, 5 (2014).

16 Dash P K, Rai R, Mahato AK, Gaikwad K & Singh NK, Transcriptome landscape at different developmental stages of a drought tolerant cultivar of flax (*Linum usitatissimum*). *Front Chem*, 5 (2017).

17 Wang Z, Hobson N, Galindo L, Zhu S, Shi D, McDill J, Yang L, Hawkins S, Neutelings G, Datla R, Lambert G, Galbraith DW, Grassa CJ, Geraldes A, Cronk QC, Cullis C, Dash PK, Kumar PA, Cloutier S, Sharpe AG, Wong GK, Wang J & Deyholos MK, The genome of flax (*Linum usitatissimum*) assembled de novo from short shotgun sequence reads. *Plant J*, 72 (2012) 461.

18 Shivakumara TN, Sreevathsa R, Dash PK, Sheshshayee MS, Papolu PK, Rao U, Tuteja N & Udaykumar M, Overexpression of pea DNA helicase 45 (PDH45) imparts tolerance to multiple abiotic stresses in chili (*Capsicum annuum* L.). *Sci Rep*, 7 (2017).

19 Kesiraju K, Tyagi S, Mukherjee S, Rai R, Singh NK, Sreevathsa R & Dash PK, An apical meristem-targeted in planta transformation method for the development of transgenics in flax (*Linum usitatissimum*): Optimization and validation. *Front Plant Sci*, 11 (2021).

20 Dash PK, Gupta P, Jailani AK & Rai R, Hydropenia induces expression of drought responsive genes ( DRGs ) erd1, hat, plD- δ , and zfa in *Linum usitatissimum* L . *Indian J Exp Biol*, 56 (2018) 743.

21 Gupta P & Dash PK, Precise method of in situ drought stress induction in flax ( *Linum usitatissimum* ) for RNA isolation towards down-stream analysis. *An Agric Res*, 36 (2015) 10.

22 Dash PK, Gupta P & Rai R, Hydroponic method of halophobic response elicitation in flax (*Linum usitatissimum*) for precise down- stream gene expression studies. *Int J Trop Agric*, 33 (2015) 1079.

23 Gupta P, Rai R, Vasudev S, Yadava D & Dash PK, Ex-foliar application of glycine betaine and its impact on protein, carbohydrates and induction of ROS scavenging system during drought stress in flax (*Linum usitatissimum*). *J Biotechnol*, 337 (2021) 80.

24 Murray MG & Thompson WF, Rapid isolation of high molecular weight plant DNA. *Nucleic Acids Res*, 8 (1980) 4321.

25 Dash PK, Gupta P, Panwar BS & Rai R, Isolation, cloning and characterization of phlB gene from an Indian strain of Gram negative soil bacteria Pseudomonas fluorescens. *Indian J Exp Biol*, 58 (2020) 412.

26 Gupta P, Rai R & Dash PK, Isolation, cloning and characterization of phlA gene from an indigenous Pseudomonas strain from Indian soil. *Int J Trop Agric*, 33 (2015) 3195.

27 Gedam PA, GK K, Ramakrishnan RS, Sharma R, Chaturvedi A & Singh VP, Ethylene induced stay-green gene expression regulates drought stress in wheat. *Indian J Exp Biol*, 59 (2021) 761.

28 Silambarasan V, Gayathiri S, Deepalakshmi G, Banu MS, Nithya V & Archunan G, Cloning and sequencing of α-2u globulin of rat preputial gland to assess its longevity in the context of developing an effective rodent trap. *Indian J Biochem Biophys*, 56 (2019) 433.

29 Chen W, Jing X, Sun L, Cai HC & Wang Y, Genome cloning and genetic diversity of apple chlorotic leaf spot virus. *Indian J Biochem Biophys*, 56 (2019) 514.

30 Chen H, Nelson RS & Sherwood JL, Enhanced recovery of transformants of *Agrobacterium tumefaciens* after freeze-thaw transformation and drug selection. *Biotechniques*, 16 (1994) 664.

31 Zhang Y, I-TASSER: Fully automated protein structure prediction in CASP8. *Proteins Struct Funct Bioinforma*, 77 (2009) 100.

32 Toppo AL, Yadav M, Dhaga S, Ayothiraman S & Eswari JS, Molecular docking and ADMET analysis of synthetic statins for HMG-CoA reductase inhibition activity. *Indian J Biochem Biophys*, 58 (2021) 127.

33 Janani DM & Usha B, In silico analysis of functional non-synonymous and intronic variants found in a polycystic ovarian syndrome (PCOS) candidate gene: DENND1A. *Indian J Biochem Biophys*, 57 (2020) 584.

34 Zaheer ZA & Sankaranarayanan K, In silico analysis of κ-theraphotoxin-Cg2a from Chilobrachys guangxiensis. *Indian J Biochem Biophys*, 57 (2020) 458.
35 Lovell SC, Davis IW, Arendall WB, de Bakker PIW, Word JM, Prisant MG, Richardson JS & Richardson DC, Structure validation by Cα geometry: ϕ, ψ and Cβ deviation. *Proteins Struct Funct Bioinforma*, 50 (2003) 437.
36 Laskowski RA, PDBsum more: new summaries and analyses of the known 3D structures of proteins and nucleic acids. *Nucleic Acids Res*, 33 (2004) 266.
37 Castrignano T, The PMDB Protein Model Database. *Nucleic Acids Res*, 34 (2006) 306.
38 Murashige T & Skoog FA, Revised medium for rapid growth and bio assays with tobacco tissue cultures. *Physiol Plant*, 15 (1962) 473.
39 Fujiyama K, Hino T, Kanadani M, Watanabe B, Jae Lee H, Mizutani M & Nagano S, Structural insights into a key step of brassinosteroid biosynthesis an d its inhibition. *Nat Plants*, 5 (2019) 589.
40 Sibanda BL, Blundell TL & Thornton JM, Conformation of β-hairpins in protein structures. *J Mol Biol*, 206 (1989) 759.
41 Hutchinson EG & Thornton JM, A revised set of potentials for β-turn formation in proteins. *Protein Sci*, 3 (1994) 2207.
42 Dash PK & Rai R, Translating the "banana genome" to delineate stress resistance, dwarfing, parthenocarpy and mechanisms of fruit ripening. *Front Plant Sci*, 7 (2016).
43 Dash PK & Rai R, Green revolution to grain revolution: Florigen in the frontiers. *J Biotechnol*, 343 (2021) 38.
44 Kamboj D, Yadav RC, Singh A & Yadav NR, Plant regeneration and *Agrobacterium*-mediated transformation in Indian mustard (*Brassica juncea* L.). *J Oilseed Brassica*, (2015) 191.
45 Sahni S, Prasad BD, Liu Q, Grbic V, Sharpe A, Singh SP & Krishna P, Overexpression of the brassinosteroid biosynthetic gene DWF4 in *Brassica napus* simultaneously increases seed yield and stress tolerance. *Sci Rep*, 6 (2016) 28298.
46 Fujita S, Ohnishi T, Watanabe B, Yokota T, Takatsuto S, Fujioka S, Yoshida S, Sakata K & Mizutani M, *Arabidopsis* CYP90B1 catalyses the early C-22 hydroxylation of $C_{27}$, $C_{28}$ and $C_{29}$ sterols. *Plant J*, 45 (2006) 765.